

Analyst

Accepted Manuscript



This is an *Accepted Manuscript*, which has been through the Royal Society of Chemistry peer review process and has been accepted for publication.

Accepted Manuscripts are published online shortly after acceptance, before technical editing, formatting and proof reading. Using this free service, authors can make their results available to the community, in citable form, before we publish the edited article. We will replace this *Accepted Manuscript* with the edited and formatted *Advance Article* as soon as it is available.

You can find more information about *Accepted Manuscripts* in the [Information for Authors](#).

Please note that technical editing may introduce minor changes to the text and/or graphics, which may alter content. The journal's standard [Terms & Conditions](#) and the [Ethical guidelines](#) still apply. In no event shall the Royal Society of Chemistry be held responsible for any errors or omissions in this *Accepted Manuscript* or any consequences arising from the use of any information it contains.

Submitted to *Analyst* April 2015

Investigating Carbohydrate Isomers by IMS-CID-IMS-MS: Precursor and Fragment Ion Cross-sections

M. M. Gaye, R. Kurulugama,[‡] and D. E. Clemmer*

Department of Chemistry, Indiana University, Bloomington, IN 47405

Abstract

Ion mobility spectrometry techniques (IMS and IMS-IMS) combined with collision-induced dissociation (CID) and mass spectrometry (MS) are used to investigate the structures of singly-lithiated carbohydrate isomers. With the exception of some favorable cases, IMS-MS analyses of underivatized carbohydrates reveal that most isobaric precursor ions have similar collision cross sections (ccs). In contrast, ccs values for isomeric fragment ions obtained by IMS-CID-IMS-MS analysis are often different, and thus appear to be useful as a means of distinguishing the isomeric precursors. We report values of ccs (in He) for precursor- and associated-fragment ions for three monosaccharide isomers (glucose, galactose and fructose), ten disaccharide isomers (sucrose, leucrose, palatinose, trehalose, cellobiose, β -gentiobiose, isomaltose, maltose, lactose and melibiose), and three trisaccharide isomers (raffinose, melezitose and maltotriose). These values are discussed as a means of differentiating precursor carbohydrates.

[‡]Present address: Agilent Technologies, Santa Clara, CA 95501

*To whom the correspondence should be addressed. E-mail: clemmer@indiana.edu

Keywords: ion mobility, electrospray ionization mass spectrometry, collision-induced dissociation, carbohydrate, isomer

Introduction

High-throughput, structural characterization of carbohydrates is proving to be challenging. In part, this is because unlike linear chains of nucleic or amino acids (associated with DNA and protein sequences), carbohydrates may be made up from 20 common monosaccharide units that may be linked at five potential positions on each saccharide ring; additionally, there are two possible anomeric configurations of the linkages, some units have different ring sizes (e.g., furanose has five carbons in its ring, while pyranose has six), and numerous modifications can occur on the monomeric unit (e.g., sulfation and phosphorylation).^{1,2} In addition to the intrinsic complexity, often only limited amounts of samples may exist (i.e., a few μg , or less), and when available samples may be comprised of mixtures of closely related species such as isomers. In favorable cases, detailed three-dimensional geometric assignments of carbohydrate structures can be obtained by nuclear magnetic resonance (NMR) or crystallography.^{3,4} However, NMR typically requires milligrams of samples, is of limited utility for mixture analysis, and is not suitable for high-throughput analyses; and, crystallography requires a crystal, either of the isolated carbohydrate or a crystalized region of the molecule as it interacts with a protein or other species that is also crystalized.⁴

Advances in ionization techniques have made it possible to investigate carbohydrate structures by a range of mass spectrometry (MS) and associated separation techniques. MS techniques are extremely sensitive, making it possible to carry out experiments with vanishingly small quantities. Moreover, these techniques are well-suited for mixture analysis and can be applied in a high-throughput fashion. In the present work, the structures of carbohydrate precursor and fragment ions are

1
2
3 investigated by a combination of ion mobility spectrometry (IMS) and MS techniques.
4
5 Because an ion's mobility depends on its shape, this combination of techniques is
6
7 proving to be valuable for discerning between different isomeric forms.^{5,6}
8
9

10 The studies presented below use collision-induced dissociation (CID) which
11 allows us to use differences in fragment-ion structures to identify different disaccharide
12 and trisaccharide isomers. We have chosen precursors comprised of a small number of
13 monosaccharide units, and having an isomeric affiliation with one another. These are
14 shown in Scheme 1. Sucrose, leucrose and palatinose are disaccharides of glucose and
15 fructose, linked by an α -glycosidic bond. They differ only in linkage position (1-2, 1-5
16 and 1-6, respectively, where the first number indicates the position on the
17 monosaccharide unit at the non-reducing end and the second number indicates the
18 linkage position on the monosaccharide unit at the reducing end). Five other
19 disaccharides (trehalose, cellobiose, β -gentiobiose, isomaltose and maltose) are
20 comprised solely of glucose units. These differ by the linkage anomericity, linkage
21 position, or both. Two additional disaccharides, lactose and melibiose are comprised of
22 galactose and glucose monomer units and differ from one another by linkage position
23 and anomericity. Raffinose, melizitose and maltotriose are trisaccharides comprised of
24 glucose and/or galactose and/or fructose residues. Additionally, cross sections for the
25 intact monomers of glucose, galactose, and fructose, are reported as well.
26
27
28
29
30
31
32
33
34
35
36
37
38
39
40
41
42
43
44
45
46
47

48 This work builds on prior work using condensed-phase separation techniques
49 such as capillary electrophoresis (CE) or high pressure liquid chromatography (often
50 following sequential exoglycosidase digestion) along with multi-stage mass
51 spectrometry (MS^n) for the elucidation of carbohydrate isomeric structures.⁷⁻¹⁰
52
53
54
55
56
57
58
59
60

1
2
3 Carbohydrate fragment ions can be produced by CID,^{9,11,12} electron capture (or transfer)
4 dissociation [ECD, (or ETD)],¹³⁻¹⁶ and vacuum ultraviolet photodissociation (VUVPD).¹⁷⁻
5
6
7
8
9
10
11
12
13
14
15
16
17
18
19
20
21
22
23
24
25
26
27
28
29
30
31
32
33
34
35
36
37
38
39
40
41
42
43
44
45
46
47
48
49
50
51
52
53
54
55
56
57
58
59
60

¹⁹ Fragmentation via CID primarily occurs via glycosidic bond cleavage; ECD, ETD and VUVPD produce additional cross-ring fragments useful for linkage position information.^{9,11-14,16-19} Often, multi-stage MSⁿ is necessary because fragment ions after MS² may be isobaric²⁰ such that no specific structural information can be obtained. Although powerful algorithms have been developed to overcome this difficulty,^{9,21} there is still a need for complementary technologies carbohydrate analysis. Below, we explore IMS as a means of complementing MS-based structural assignments.

A number of recent studies have used IMS-MS techniques to investigate carbohydrate structures.^{19,22-35} Early on, Liu *et al.*²², established that isomeric fragment ions (originating from isomeric precursor ions) could be distinguished based on differences in mobilities through N₂ buffer gas. Lee *et al.* used a combination of IMS with VUVPD to characterize a mixture of seven disaccharides by using the extracted fragment drift time distributions of specific fragment ions that were unique to each disaccharide.¹⁹ Finally, the present work is also closely related to elegant studies by Hill's³⁴ and Eyers's³⁶ groups, using different combinations of IMS-MS and CID methodologies. Overall, our efforts in combination with the studies conducted by Hill, Eyers, and coworkers,^{34,36} are of significance towards the establishment of a ccs library of carbohydrate precursor and fragment ions, which in due course will lead to high-throughput sequencing capabilities for carbohydrates.

Experimental section

1
2
3 Materials and sample preparation. Thirteen carbohydrates (all in the D(+) form)
4
5 were purchased from Sigma-Aldrich (St. Louis, MO). Three of these were the
6
7 monosaccharides glucose, fructose and galactose; eight were the disaccharides
8
9 sucrose, palatinose, leucrose, maltose, trehalose, lactose, cellobiose, and β -
10
11 gentiobiose; and, two were the trisaccharides melezitose, and raffinose. The
12
13 disaccharides, isomaltose and melibiose as well as the trisaccharide maltotriose were
14
15 obtained from Santa Cruz Biotechnology (Dallas, TX). All carbohydrates were used
16
17 directly as purchased. The structures for all of these molecules are depicted in Scheme
18
19 1. Solutions for electrospray were prepared as $0.25 \text{ mg}\cdot\text{ml}^{-1}$ in a 90:10 (vol.%)
20
21 water:acetonitrile and 2.0 mM LiCl.
22
23
24
25
26

27 IMS-MS and IMS-CID-IMS-MS measurements. Theoretical and experimental
28
29 aspects of an IMS-MS measurement as well as the home-built IMS-time-of-flight (TOF)
30
31 MS instrument used in this study are described elsewhere.^{5,37-40} A schematic diagram of
32
33 the instrument is shown in Figure 1. The instrument consists of an electrospray
34
35 ionization (ESI) source coupled with an automatic injection system (NanoMate TriVersa,
36
37 Advion, Ithaca, NY), a two meter long drift tube (D1 and D2) that is equipped with an ion
38
39 selection and activation region, and a TOF mass analyzer. In a typical IMS-MS
40
41 experiment, ions are accumulated in the source ion funnel (F1) and periodically pulsed
42
43 into the drift tube as a narrow packet of ions ($150 \mu\text{s}$ wide), where they are separated
44
45 according to their mobilities in He buffer gas. Ions exit the drift tube through a
46
47 differentially pumped region and are extracted into the source region of a reflectron
48
49 geometry TOF for mass analysis and detection. In the present experiment, the drift tube
50
51 is filled with ~ 2.3 Torr of He at 294 K and operated under a uniform electric field of 9.6
52
53
54
55
56
57
58
59
60

1
2
3 V·cm⁻¹. The source ion funnel is operated at 15 V·cm⁻¹ and ~1.69 Torr of He; the back
4
5 (F3, Figure 1) and mid (F2, Figure 1) ion funnels are operated at 12 V·cm⁻¹ and ~2.25
6
7 Torr of He. A radio frequency field ranging from 390 to 440 kHz with a peak-to-peak
8
9 amplitude of 120 to 140 V_{p-p} is applied to all three ion funnels.
10
11

12
13 A unique feature of this instrumentation is the ability to select and activate
14
15 mobility-separated ions. In an IMS-CID-IMS-MS experiment, the two parts of the drift
16
17 tube D1 and D2 are operated independently. That is, a first pulse (G1, Figure 1)
18
19 introduces all ions in D1 and a synchronized second pulse (G2), applied at the entrance
20
21 of the mid ion funnel, allows only a narrow distribution of ions with specified mobilities
22
23 into F2. For all carbohydrates presented in Table 1 the precursor ion [M+Li]⁺ is selected
24
25 at the entrance of the second drift region, after ~72 cm of mobility separation. The
26
27 mobility-selected ions are subsequently fragmented in the ion activation region (IA2,
28
29 Figure 1, comprised of two lenses which are spaced ~0.3 cm apart). The resulting
30
31 fragments are mobility separated in the second drift tube, region D2 prior to mass
32
33 analysis. Fragmentation studies are performed by raising the field across IA2 from 12
34
35 V·cm⁻¹ to 530 V·cm⁻¹ for disaccharides and from 12 V·cm⁻¹ to 615 V·cm⁻¹ for
36
37 trisaccharides. IMS-CID-IMS-MS has been previously used in our group for the analysis
38
39 of peptide and protein fragment ions.⁴¹ We report here the application of this technique
40
41 to the characterization of carbohydrate isomeric ions.
42
43
44
45
46
47

48
49 The IMS-CID-IMS-MS process primary produces glycosidic bond cleavages
50
51 named Y_n, C_n, B_n and Z_n, according to Domon and Costello nomenclature,⁴² n
52
53 representing the number of rings retained in the structure. Y_n and Z_n fragments
54
55 correspond to the reducing end of a carbohydrate with the glycosidic oxygen (Y_n) and
56
57
58
59
60

without the glycosidic oxygen (Z_n) respectively. Likewise, C_n and B_n fragment ions refer to the non-reducing end of a carbohydrate with and without the glycosidic oxygen respectively. Y, C, B and Z fragmentation patterns are shown in Scheme 2. Cross-ring fragments are also observed in the case of disaccharides; cross-ring fragments retaining the reducing end are named $^{ij}A_n$ and cross-ring fragments retaining the non-reducing end are named $^{ij}X_n$. The superscript "i,j" indicates carbons after which cleavages occur. In the present experiment all fragment ions are lithiated and the notation Y/C indicates ions that are either Y or C fragments (likewise for B/Z).

Experimental collision cross sections. The total time required for an ion to traverse through the instrument is equivalent to the sum of the drift time, flight time, and the time required to travel through the instrument's interface regions. For a uniform electric field applied along the drift region, collision cross sections can be calculated directly from the drift time distributions (through the entire instrument) using Equation 1,⁴³

$$\Omega = \frac{(18\pi)^{1/2}}{16} \frac{ze}{(k_b T)^{1/2}} \left[\frac{1}{m_I} + \frac{1}{m_B} \right]^{1/2} \frac{t_D E}{L} \frac{760}{P} \frac{T}{273.2} \frac{1}{N} \quad (1),$$

where ze , k_b , m_I , and m_B refer to the charge of the ion, Boltzmann's constant, the mass of the ion, and the mass of the buffer gas (helium in these experiments). The variables t_D , E , L , P , T , and N correspond to the drift time, electric field, drift tube length, buffer gas pressure and temperature, and the neutral number density of the buffer gas, respectively. The final term in the equation normalizes the mobility to standard temperature and pressure (STP). Due to the presence of the two funnels at F2 and F3

1
2
3 which are operated at a relatively high field, cross section determination through the
4
5 entire instrument often involves a simple calibration technique for which the individual
6
7 drift times for well-characterized ions (typically bradykinin and polyalanine) are used for
8
9 calibration. The calibration can be tested using a highly rigorous approach for
10
11 determining cross sections involving scanning across a peak by varying the application
12
13 time of the gates G1 and G2. The delay time applied at G2 in order to select a specific
14
15 precursor ion defines its drift time. The conversion to cross sections of selected ions is
16
17 then accomplished with no additional corrections through equation 1 using the
18
19 appropriate drift lengths. Similarly the cross sections of fragment ions can be
20
21 determined through the second drift region.
22
23
24
25
26
27
28

29 **Results and discussion**

30
31 IMS-CID-IMS-MS analyses of lithiated carbohydrates. An example spectrum resulting
32
33 from an IMS-CID-IMS-MS experiment performed on the trisaccharide melezitose is
34
35 shown in Figure 2. Ions are observed over a range of m/z and drift time values: from
36
37 169 m/z to 511 m/z ; and, from 9.9 ms to 13.5 ms in the drift time dimension. The
38
39 precursor ion $[M+Li]^+$ at 511 m/z is the most intense feature. The most intense
40
41 fragments are Y_2/C_2 and B_2/Z_2 at respectively 349 m/z and 331 m/z with associated drift
42
43 times of 11.9 ms and 11.8 ms. Both Y_2/C_2 and B_2/Z_2 fragments correspond to the loss of
44
45 one monosaccharide unit by glycosidic bond cleavage. A loss of a disaccharide by
46
47 cleaving one of the two glycosidic bonds gives rise to peaks at 187 m/z ($t_D = 10.3$ ms)
48
49 and 169 m/z ($t_D = 9.9$ ms). Finally, the feature at 187 m/z with an associated drift time of
50
51 12 ms (Figure 2) is the consequence of the fragmentation of the Y_2/C_2 ion in the back of
52
53
54
55
56
57
58
59
60

1
2
3 our home-built instrument (Figure 1). This feature is clearly resolved in the mobility
4 dimension from the isobaric fragment Y_1/C_1^* ($187\ m/z$, $t_D = 10.3\ ms$) generated in the
5 instrument mid funnel (F2). The star symbol on Y_1/C_1^* indicates the possibility of an
6 additional fragment assignment (Y_2-Z_1/C_2-B_1 isobaric of Y_1/C_1), originating from
7 breaking two glycosidic bonds simultaneously to yield the monosaccharide unit in the
8 middle of the trisaccharide sequence.
9
10
11
12
13
14
15
16

17
18 In the case of the disaccharide β -gentiobiose, fragments resulting from both
19 glycosidic bond cleavage and cross-ring fragments are produced. Figure 2 illustrates
20 the 2D-plot and associated mass spectrum resulting from the IMS-CID-IMS-MS
21 experiment completed on β -gentiobiose. The precursor ion $[M+Li]^+$ ($349\ m/z$, $t_D = 11\ ms$)
22 is the feature with the largest intensity in both the 2D-plot and the mass spectrum
23 (Figure 2). The main fragment resulted from glycosidic bond cleavage with retention of
24 the glycosidic oxygen (Y_1/C_1 , $187\ m/z$, $t_D = 9.3\ ms$). The Y_1/C_1 fragment ion originating
25 from β -gentiobiose is representative of one monosaccharide unit and interestingly the
26 structure obtained here has a shorter drift time (1 ms difference) than the corresponding
27 isobaric fragment ion obtained from the trisaccharide melezitose. Similarly, the fragment
28 ion resulting from glycosidic cleavage without retention of the glycosidic oxygen (B_1/Z_1 ,
29 $169\ m/z$) appeared at a shorter time ($t_D = 9\ ms$) than its counterpart ($t_D = 9.9\ ms$)
30 resulting from melezitose fragmentation. In the case of melezitose and β -gentiobiose,
31 both Y_1/C_1 and B_1/Z_1 fragments are made of a glucose unit but differ by the type of
32 glycosidic linkage that was broken (α 1-2 and β 1-6 respectively). The fact that isobaric
33 fragments resulting from β -gentiobiose or melezitose have different drift times suggests
34 that these two fragments retained linkage information from the precursor ion, resulting in
35
36
37
38
39
40
41
42
43
44
45
46
47
48
49
50
51
52
53
54
55
56
57
58
59
60

1
2
3 different structure(s) and/or conformer(s). Thus, population of fragment ions are used to
4
5 distinguish carbohydrate isomers. Structural similarities and differences between
6
7 fragment ions are further investigated by examining their corresponding mobility
8
9 profiles. Additional fragments are reported (Figure 2): $[M-H_2O+Li]^+$ resulting from the
10
11 loss of water ($331\ m/z$, $t_D=10.7\ ms$) as well as cross-ring fragments $^{2,4}X_1$ ($289\ m/z$, $t_D =$
12
13 $10.1\ ms$) and $^{1,4}A_1/^{0,3}X_1$ ($259\ m/z$, $t_D = 9.8\ ms$). Lastly, fragment ions with an associated
14
15 drift time of 11 ms (Figure 2, $169\ m/z$ and $187\ m/z$) resulting from fragmentation in the
16
17 back of the instrument are resolved from the fragment ions of interest Y_1/C_1 ($t_D =9.3\ ms$)
18
19 and B_1/Z_1 ($t_D =9\ ms$).
20
21
22
23
24
25
26

27 Disaccharide mobility distributions for delineation between isomers. The mobility
28
29 distribution of an ion is generated from the 2D-plot by integrating all m/z bins (centered
30
31 on the ion m/z) across a narrow range for each drift time bin. Collision cross sections
32
33 (ccs in \AA^2) are derived from the mobility equation as described elsewhere.^{5,44} Figure 3
34
35 depicts mobility profiles of lithiated disaccharide ions.
36
37
38

39 **Precursor ion $[M+Li]^+$ ($349\ m/z$).** Maltose, β -gentiobiose, cellobiose and
40
41 trehalose are isomers made of two glucoses that differ by only the type of glycosidic
42
43 linkage (Table 1). Mobility distributions for maltose, β -gentiobiose and trehalose
44
45 precursor ions display a single sharp feature. Interestingly, the mobility profile of
46
47 cellobiose shows a broader feature. A similar trait is observed in the case of precursor
48
49 ions lactose and melibiose. That is, the mobility distribution for lactose is broader than
50
51 the mobility distribution of melibiose (data not shown). Both lactose and melibiose are
52
53 made of galactose and glucose, the former having a β 1-4 type of glycosidic linkage (α
54
55
56
57
58
59
60

1-6 for melibiose, Table 1). The observed broadening of the mobility feature for a disaccharide with a β 1-4 linkage type suggests that this type of linkage is likely to give rise to multiple conformations in the gas phase. An exhaustive study of the conformational space occupied by carbohydrate isomers is beyond the scope of this paper and will be addressed in the future by using annealing techniques such as IMS-IMS-MS. Cellobiose and β -gentiobiose precursor ions have similar ccs (respectively 108.6 \AA^2 and 108.1 \AA^2) and cannot be distinguished in the present case. In contrast, trehalose and maltose precursor ions have ccs, not only different from each other, but also different from cellobiose and β -gentiobiose. Trehalose is the most compact ion with a ccs centered at 105.1 \AA^2 and maltose is the most elongated ion with a ccs centered at 110.6 \AA^2 . As result, the two isomers trehalose and maltose can be distinguished based on their respective mobility distributions.

Mobility distributions for ions resulting from the neutral loss of a water molecule from the precursor ion after being subjected to IMS-CID-IMS-MS ($[M-H_2O+Li]^+$, m/z 331) are depicted for cellobiose and trehalose (Figure 3). This ion was not observed after fragmentation of the precursor ion trehalose and was of very low intensity for the precursor ion maltose. The mobility distribution of $[M-H_2O+Li]^+$ originating from cellobiose displays a single feature at 105.7 \AA^2 . Interestingly, the mobility distribution of $[M-H_2O+Li]^+$ arising from β -gentiobiose displays multiple features: the main feature is centered at 105.7 \AA^2 , two shoulders at 108.2 \AA^2 and 110.0 \AA^2 and one more compact feature at 98.7 \AA^2 . The features at 105.7 \AA^2 , 108.2 \AA^2 and 110.0 \AA^2 most likely result from different conformers of this fragment. The peak at 98.7 \AA^2 could result from a

1
2
3 neutral loss of water at an alternate location of the carbohydrate, and as a result an
4
5 additional structure of this ion in the gas phase is observed.
6
7

8 **Fragment ions with retention of the glycosidic oxygen.** Mobility profiles of
9
10 fragments Y_1/C_1 (m/z 187) originating from glucose-only disaccharides (Figure 3)
11
12 present a trend similar to the one observed for the precursor ions. It is interesting to
13
14 note that the mobility distribution of fragment ions are broader than in the case of
15
16 precursor ions. A possible explanation of this phenomenon is that for a given m/z , the
17
18 charge carried by the lithium atom is either retained by the reducing end (Y fragment) or
19
20 retained by the non-reducing end (C fragment), hence yielding a greater number of
21
22 possible conformers than for the corresponding precursor ion. The delineation between
23
24 isobaric Y and C fragment ions will allow unambiguous sequencing of carbohydrate
25
26 isomers and is currently investigated by our group.
27
28
29
30
31

32 **Fragment ions without the glycosidic oxygen.** B_1/Z_1 fragments (m/z 169,
33
34 Figure 3) originating from glucose disaccharides isomers have unique mobility
35
36 distributions comprised of multiple features. The fragment ion resulting from the IMS-
37
38 CID-IMS-MS experiment performed on maltose (m/z 169, Figure 3, bottom trace)
39
40 displays two main features at respectively 89.2 \AA^2 and 91.0 \AA^2 , the latter being greater
41
42 in intensity; and a minor elongated feature centered at 94.6 \AA^2 . In the case of fragment
43
44 originating from β -gentiobiose (Figure 3, second trace from bottom), the most compact
45
46 feature (86.7 \AA^2) is greater in intensity than the more elongated one (90.0 \AA^2);
47
48 additionally, two minor features at 92.4 \AA^2 and 94.2 \AA^2 are present. Similar minor
49
50 features (92.4 \AA^2 and 93.6 \AA^2) are also visible on the mobility distribution of the B_1/Z_1
51
52 fragment originating from cellobiose (Figure 3, second trace from top); the two main
53
54
55
56
57
58
59
60

1
2
3 features (87.0 \AA^2 and 88.8 \AA^2) are of equal intensities. Finally, fragment originating from
4
5 trehalose (Figure 3, top trace) generated a mobility profile with a compact feature at
6
7 87.3 \AA^2 , a more elongated feature at 89.2 \AA^2 with an intensity ~ 2.5 greater than the
8
9 compact one and a minor feature at 94 \AA^2 . Collision cross sections for the main features
10
11 of B/Z fragment ions initiated by trehalose and cellobiose are close but the relative
12
13 intensities in which these features exist are drastically different. For this reason,
14
15 trehalose and cellobiose isomers can be distinguished based on the mobility
16
17 distributions of their respective B/Z fragment ions. B and Z fragment ions are oxonium
18
19 ions formed respectively at the reducing end of a carbohydrate (B fragment) or the non-
20
21 reducing end of a carbohydrate (Z fragment).³⁶ These two different structures most
22
23 likely generated different conformations or population of conformations upon binding to
24
25 a lithium atom. As a consequence, the two main features observed in the four
26
27 disaccharide fragments could be respectively representative of B and Z ions. Further
28
29 studies are underway to distinguish B and Z ions.
30
31
32
33
34
35

36 **Glucose-fructose disaccharides.** Mobility profiles associated with sucrose,
37
38 leucrose and palatinose, which differ only by the type of glycosidic bond, are depicted in
39
40 Figure 4. All three precursor ions $[M+Li]^+$ (m/z 349) display a single sharp feature.
41
42 Sucrose and leucrose have similar ccs (104.5 \AA^2 and 104.6 \AA^2 , respectively) while
43
44 palatinose has a larger structure (106.4 \AA^2). Interestingly, mobility distributions of Y_1/C_1
45
46 fragment ions (m/z 187, Figure 4) are different for all three isomers. The fragmentation
47
48 of palatinose (Figure 4, bottom trace) yielded two features; a compact (low intensity)
49
50 feature with an associated ccs of 85.4 \AA^2 and a more elongated one at 89.7 \AA^2 . The
51
52 mobility distribution of the Y_1/C_1 fragment originating from sucrose displays a single
53
54
55
56
57
58
59
60

1
2
3 peak centered at 89.5 \AA^2 (Figure 4, top trace). Although the ccs value associated with
4 fructose fragment ion is close to the one measured for the main feature of the
5 palatinose Y_1/C_1 ion, the two ions can be distinguished because the fragmentation of
6 palatinose generated an additional conformation or ensemble of conformations (85.4 \AA^2 ,
7 Figure 4, bottom trace) not observed when sucrose is fragmented. The mobility profile
8 of the Y_1/C_1 fragment ion obtained from leucrose presents a single feature (88.0 \AA^2 ,
9 Figure 4, middle trace) and is distinct from the two other fragment ion mobility profiles.

10
11
12
13
14
15
16
17
18
19
20 The delineation between sucrose, leucrose and palatinose is further improved
21 when the mobility distribution of B_1/Z_1 fragment ions are considered (m/z 169, Figure 4).
22 The main peak originating from the fragmentation of sucrose is saturated (m/z 169, 86.5
23 \AA^2 , Figure 4, top trace). That is, sucrose fragmentation upon IMS-CID-IMS-MS was
24 more efficient (yielded more intense features) in comparison with leucrose, palatinose
25 and the other disaccharides examined in the present work. In addition a very low
26 intensity feature is observed at 88.9 \AA^2 . The mobility distribution of the B_1/Z_1 ion initiated
27 by leucrose fragmentation (m/z 169, Figure 4, middle trace) displays two features at
28 respectively 86.3 \AA^2 and 88.7 \AA^2 ; the most elongated one being three times higher in
29 intensity than the more compact one. Lastly, the B_1/Z_1 fragment ion originating from
30 palatinose (m/z 169, Figure 4, bottom trace) shows a broad distribution centered at 87.3
31 \AA^2 and an unresolved shoulder at $\sim 89 \text{ \AA}^2$. Interestingly, the population of ions observed
32 at $\sim 89 \text{ \AA}^2$ in the case of B_1/Z_1 fragment ion yielded by palatinose is also observed in the
33 case of leucrose (88.7 \AA^2) and sucrose (88.9 \AA^2); this population of ions is likely to be
34 specific to either B or Z ions. As we discussed above for glucose disaccharide isomers,
35 multiple features observed on the mobility profiles of B_1/Z_1 fragment ions are likely to be
36
37
38
39
40
41
42
43
44
45
46
47
48
49
50
51
52
53
54
55
56
57
58
59
60

1
2
3 representative of unique population of conformers for B and Z fragment ions
4
5 respectively. In summary, sucrose, leucrose and palatinose isomers are unambiguously
6
7 distinguished based on the mobility distribution of their respective fragment ions
8
9 generated by IMS-CID-IMS-MS.
10
11

12 Mobility distributions of trisaccharide isomers. Mobility profiles of raffinose,
13
14 melezitose and maltotriose precursor ions $[M+Li]^+$ (m/z 511) are depicted in Figure 5.
15
16 The mobility distribution of melezitose precursor ion (Figure 5) displays a unique feature
17
18 centered at 132.6 \AA^2 which can be differentiated from the single feature in mobility
19
20 profiles of both raffinose (137.4 \AA^2) and maltotriose (138.0 \AA^2) precursor ions. The
21
22 middle panel of Figure 5 illustrates mobility distributions of Y_2/C_2 fragment ions (m/z
23
24 349) obtained by IMS-CID-IMS-MS analysis of raffinose, melezitose and maltotriose
25
26 precursor ions. Interestingly, the mobility profile of the Y_2/C_2 fragment ion, originating
27
28 from maltotriose fragmentation (m/z 349, Figure 5, bottom trace), shows two features.
29
30 The main feature has an associated ccs of 120.3 \AA^2 , and the more compact feature
31
32 (approximately ten times lower in intensity) has a ccs centered at 116.7 \AA^2 . Because the
33
34 Y_2/C_2 ion generated by the fragmentation of raffinose (m/z 349, Figure 5, top trace)
35
36 presents a single feature at 120.3 \AA^2 , raffinose and maltotriose can be distinguished in
37
38 the present case. Melezitose Y_2/C_2 fragment ion has a more compact structure (m/z
39
40 349, 115.6 \AA^2 , Figure 5, middle trace) than the structures obtained for fragment ions
41
42 originating from raffinose and maltotriose.
43
44
45
46
47
48
49

50
51 As observed for disaccharide precursor ions, the mobility distribution of B/Z
52
53 fragment ions often show shoulders on the main peak. The most compact structure is
54
55 obtained for the B_2/Z_2 fragment initiated by melezitose (m/z 331, Figure 5, middle trace);
56
57
58
59
60

1
2
3 a broad distribution centered at 113.3 \AA^2 and a shoulder at $\sim 115 \text{ \AA}^2$. The mobility
4 distribution of the B_2/Z_2 ion originating from the fragmentation of raffinose displays
5 multiple features (m/z 331, Figure 5, top trace); a main feature (118.5 \AA^2) and three
6 minor features (120.9 \AA^2 , 122.7 \AA^2 and 125.7 \AA^2). Lastly, the mobility distribution of
7 B_2/Z_2 ions arising from the fragmentation of maltotriose (m/z 331, Figure 5, bottom trace)
8 shows a single feature with an associated ccs of 118.0 \AA^2 ; interestingly, there are no
9 minor features, and therefore can be distinguished from the B_2/Z_2 ions originating from
10 raffinose.
11
12
13
14
15
16
17
18
19
20
21

22 Using complementary IMS fragment ion information to characterize precursor ion
23 isomers. Recently, Evers and coworkers have described the idea of using IMS
24 information to complement MS-based sequencing methods.³⁶ The basic idea of this
25 approach is that fragments containing specific residues and linkages cannot be
26 unambiguously identified based on MS information alone; however, these fragments
27 once formed retain elements of structure that are specific to different isomers. Thus,
28 information about their respective mobilities can be used to discriminate between
29 species having identical masses. Our data indicates a similar trend. Figure 6 depicts ccs
30 for ten disaccharide precursor ions plotted as a function of ccs for Y_1/C_1 and B_1/Z_1
31 fragment ions. Lactose, palatinose and maltose are unambiguously distinguished based
32 on the precursor ion ccs alone (along the x-axis, Figure 6). Sucrose, leucrose and
33 trehalose (similarly melibiose, β -gentiobiose, isomaltose and cellobiose), which cannot
34 be separated based on ccs of their respective precursor ions, are unequivocally
35 distinguished when ccs for fragment ions are taken into account (along the y-axis,
36 Figure 6).
37
38
39
40
41
42
43
44
45
46
47
48
49
50
51
52
53
54
55
56
57
58
59
60

1
2
3 In addition, the identity of the fragment monomeric unit (glucose, galactose or
4 fructose) as well as the type of fragment ion are represented (Figure 6). Unlike previous
5 studies, we examine here the fragmentation of carbohydrate isomers yielding isobaric
6 Y/C and B/Z fragment ions. Because of this, an ambiguity remains for the
7 comprehensive characterization of the carbohydrate building blocks. For example, the
8 data point representing the Y_1 (or C_1) fragment arising from sucrose (Figure 6) can
9 either be a glucose or a fructose unit (and reciprocally). Because this data point belongs
10 to a cluster of reported values for the ccs distribution of Y_1/C_1 fragment of disaccharides
11 made of glucose only, extending on a diagonal from trehalose to maltose, it can be
12 inferred that the obtained Y_1/C_1 fragment from sucrose is most likely the glucose
13 fragment (C_1). In a similar fashion, the localization of the data point for the C_1/Y_1
14 fragment arising from leucrose could be indicative of the presence of a fructose unit, as this
15 data point is situated outside the observed trend for glucose units. Overall, the
16 combination of precursor- and fragment ions ccs measurements, not only allow
17 delineation between carbohydrate isomers, but also shows potential as a high-
18 throughput sequencing methodology, which will be permitted by the structural
19 characterization of monomeric building blocks.

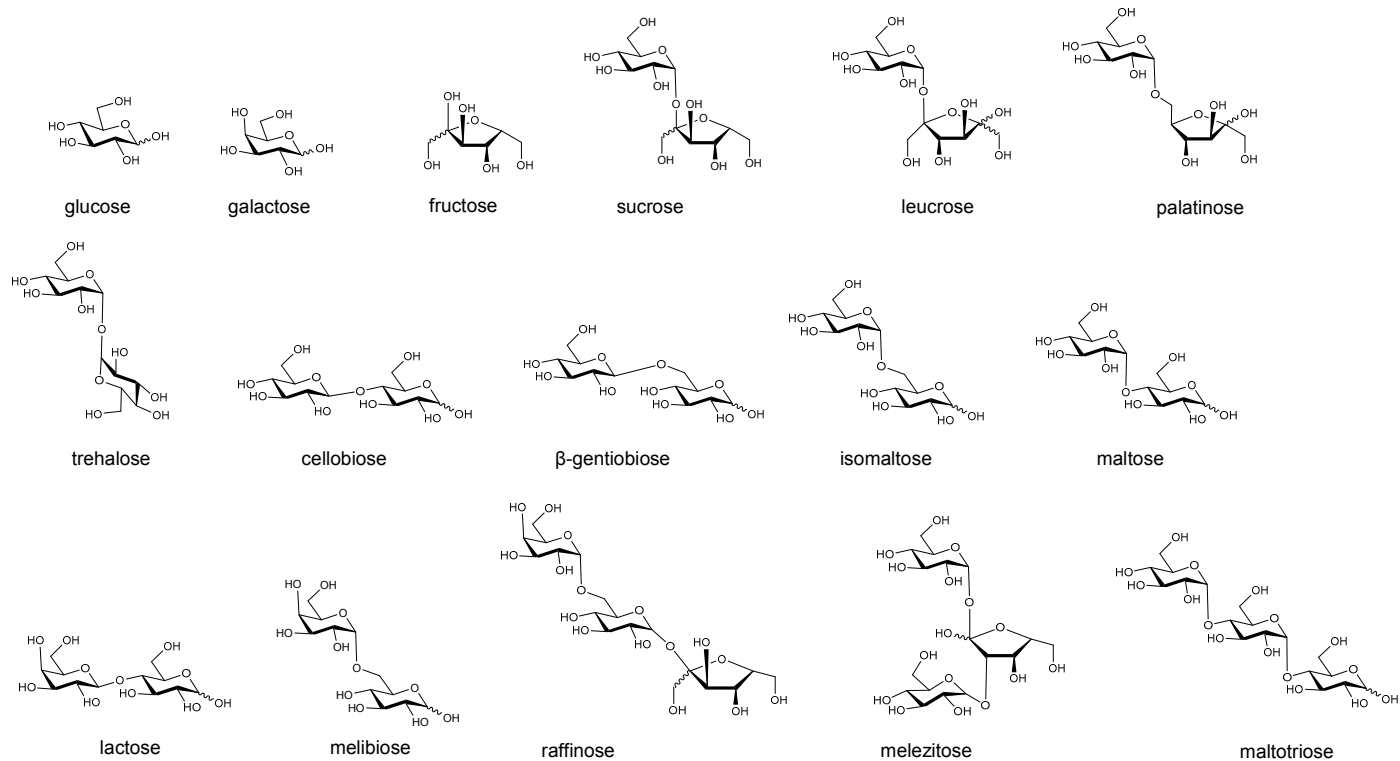
20 21 22 23 24 25 26 27 28 29 30 31 32 33 34 35 36 37 38 39 40 41 42 43 44 **Summary and conclusions**

45 Lithiated oligosaccharides were examined using IMS-MS and IMS-CID-IMS-MS.
46 In favorable cases, carbohydrate isomers can be distinguished based only on the
47 mobility distribution of the singly-lithiated precursor ion. Trehalose, maltose, melibiose,
48 lactose and melezitose are such isomers. Otherwise, a different approach is necessary.
49 The present work demonstrates that the mobility distribution of lithiated fragment ions
50
51
52
53
54
55
56
57
58
59
60

1
2
3 obtained by IMS-CID-IMS-MS can be used to distinguish between underivatized
4 carbohydrate isomers. The main fragments obtained when CID is performed in the drift
5 tube originate from the cleavage of a glycosidic bond (Y/C and B/Z fragments). In most
6 cases, the mobility profile of a fragment ion display multiple features. This set of
7 features is unique for a given precursor ion. That is, one feature exists for one precursor
8 ion but not the other, or if the same features are present (*i.e.*, at similar ccs), their
9 relative abundances vary from one isomer to another. In other words, different
10 carbohydrate isomers generate fragment ions characterized by different population of
11 conformers and/or structures. CCSs measured in He buffer gas of carbohydrate
12 precursor and fragment ions for three monosaccharide isomers, ten disaccharide
13 isomers and three trisaccharide isomers are reported. In addition, broader features were
14 observed for fragment ions in comparison with corresponding precursor ions. A
15 probable explanation for this trend is that when a glycosidic bond is broken, (1) the
16 charge is carried by either the reducing end (Y, Z fragments) or the non-reducing end
17 (C, B fragments) of the carbohydrate; and (2) for each type of fragment, the multiple
18 possible locations at which the lithium atom binds are likely to generate multiple
19 conformations. Thus, broader features, which are observed in mobility profiles of
20 fragment ions, are most likely comprised of multiple structures and/or conformers. We
21 are currently investigating means to better resolve these distributions in order to
22 delineate between isobaric Y and C (similarly B and Z) fragment ions. This
23 methodology, in combination with a concerted effort for building a ccs library of
24 precursor- and fragment-ions, holds potential for high-throughput sequencing of linear
25 carbohydrates.
26
27
28
29
30
31
32
33
34
35
36
37
38
39
40
41
42
43
44
45
46
47
48
49
50
51
52
53
54
55
56
57
58
59
60

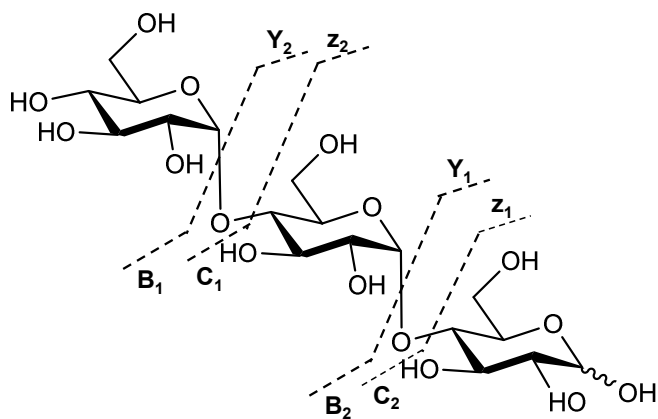
Acknowledgment

This work is supported by the National Institute of Health (NIH-5R01GM93322-2).



Scheme 1. Structure of the studied carbohydrates

1
2
3
4
5
6
7
8
9
10
11
12
13
14
15
16
17
18
19
20
21
22
23
24
25
26
27
28
29
30
31
32
33
34
35
36
37
38
39
40
41
42
43
44
45
46
47
48
49
50
51
52
53
54
55
56
57
58
59
60



Scheme 2. Types of fragment ions shown on the trisaccharide maltotriose

Table 1. Measured collision cross section for the studied carbohydrates

name	Constituents ^(a) linkage type ^(b)		collision cross section (Å ²)				
			[M+Li] ⁺ m/z 511	[Y ₂ /C ₂ +Li] ⁺ m/z 349	[B ₂ /Z ₂ +Li] ⁺ m/z 331	[Y ₁ /C ₁ +Li] ⁺ m/z 187	
raffinose	Gal-Glc-Fruc	α 1-6, β 1-2	137.4	120.3	118.5	102.9/104.1	
melezitose	Glc-Fruc-Glc	α 1-2, α 1-2	132.6	115.6	113.2	100.7	
maltotriose	Glc-Glc-Glc	α 1-4, α 1-4	138	(116.7) 120.3	118	na	
				[M+Li] ⁺ m/z 349	[M-H ₂ O+Li] ⁺ m/z 331	[Y ₁ /C ₁ +Li] ⁺ m/z 187	[B ₁ /Z ₁ +Li] ⁺ m/z 169
sucrose	Glc-Fruc	α 1-2		104.5	na	89.5	86.5
leucrose	Glc-Fruc	α 1-5		104.6	low intensity	88	(86.3) 88.7
palatinose	Glc-Fruc	α 1-6		106.4	105.6	(85.4) 89.7	87.3
trehalose	Glc-Glc	α 1-1		105.1	na	90.3	(87.3) 89.2
cellobiose	Glc-Glc	β 1-4		108.6	105.7	91.4	87/88.8
β-gentiobiose	Glc-Glc	β 1-6		108.1	105.7 (108.2)	91.7	87 (90)
isomaltose	Glc-Glc	α 1-6		108.6	low intensity	91.9	low intensity
maltose	Glc-Glc	α 1-4		110.6	low intensity	92.7	(89.2) 91
lactose	Gal-Glc	β 1-4		103	102.3	88.9	86
melibiose	Gal-Glc	α 1-6		107.4	low intensity	92.1	88.6 (91)
						[M+Li] ⁺ m/z 187	
glucose	Glc					80.8 (92.3)	
galactose	Gal					76.3/78.1 (90.3)	
fructose	Fruc					77.5/78.7 (90.3)	

(a) Monosaccharide units for the studied carbohydrates are galactose (Gal), glucose (Glc) and fructose (Fruc).

(b) Refers to the linkage between two monosaccharide units from the non-reducing end to the reducing end of the carbohydrate.

na: The fragment ion was not observed.

low intensity: The intensity of the fragment ion was too low for a collisional cross-section to be measured.

In the case of multiple features, the ccs for the least intense feature is indicated in parenthesis; ccs for two peaks of equal intensities are separated by a forward slash.

Figure Captions

Figure 1. Schematic diagram of the ion mobility/time-of-flight instrument. The primary instruments component are shown as well as the drift tube (D), ion funnels (F), ion gates (G) and the ion activation region (IA2).

Figure 2. Two-dimensional nested IMS-MS dot plots (ion intensity as a function of drift time and m/z values) obtained for the fragmentation of lithiated melezitose (**A**) and lithiated β -gentiobiose (**B**). The corresponding mass spectra are shown as an insert on the left side. Features corresponding to precursor ions (M) and fragment ions (Y_2/C_2 , B_2/Z_2 , Y_1/C_1 , B_1/Z_1 , $^{2,4}X_1$ and $^{1,4}A_1/^{0,3}X_1$) are indicated. In the case of melezitose (**A**) Y_1/C_1^* and B_1/Z_1^* indicate the existence of additional fragment assignments - originating from breaking two glycosidic bonds simultaneously to yield the monosaccharide unit in the middle of the trisaccharide sequence - for the given feature. Y_2-Z_1/C_2-B_1 are isobaric of Y_1/C_1 ; B_2-B_1/Z_2-Z_1 and Y_2-Y_1/C_2-C_1 are isobaric of B_1/Z_1 .

Figure 3. Mobility distributions, on a collision cross section (ccs) scale, of lithiated glucose disaccharides obtained by IMS-MS (precursor ions) and lithiated fragment ions obtained by IMS-CID-IMS-MS. **(a)** Precursor ions trehalose, cellobiose, β -gentiobiose and maltose. **(b)** Fragment ions at m/z 331 corresponding to the loss of water from the precursor ion for cellobiose and β -gentiobiose. **(c)** and **(d)** Fragment ions at respectively m/z 187 (Y_1/C_1) and 169 (B_1/Z_1) resulting from the glycosidic bond cleavage between the two glucose units of trehalose, cellobiose, β -gentiobiose and maltose.

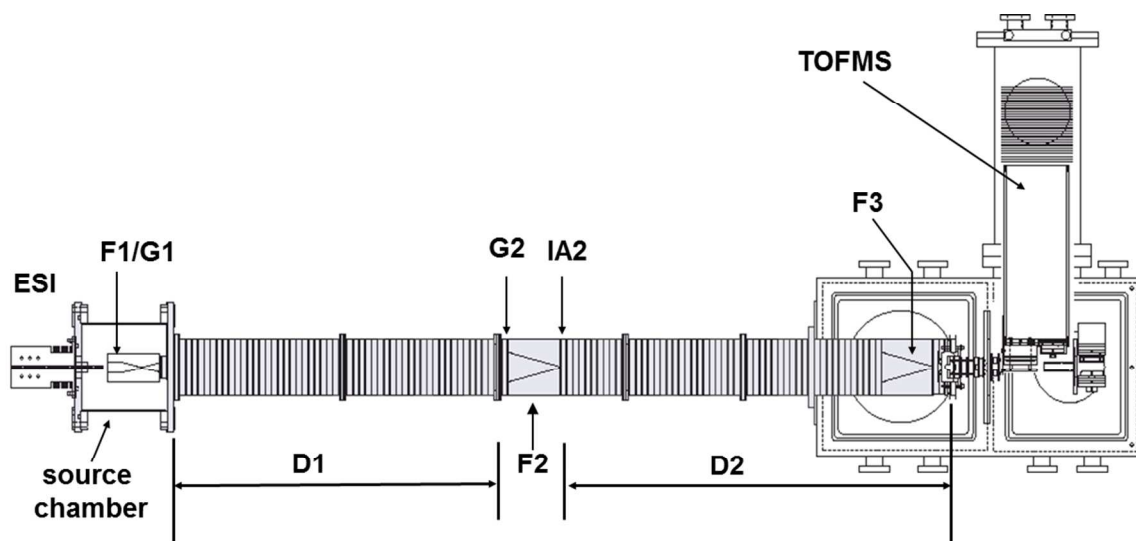
Figure 4. Mobility distributions of lithiated sucrose (top trace), leucrose (middle trace) and palatinose (bottom trace). **(a)** Precursor ions $[M+Li]^+$ (m/z 349) are obtained by IMS-

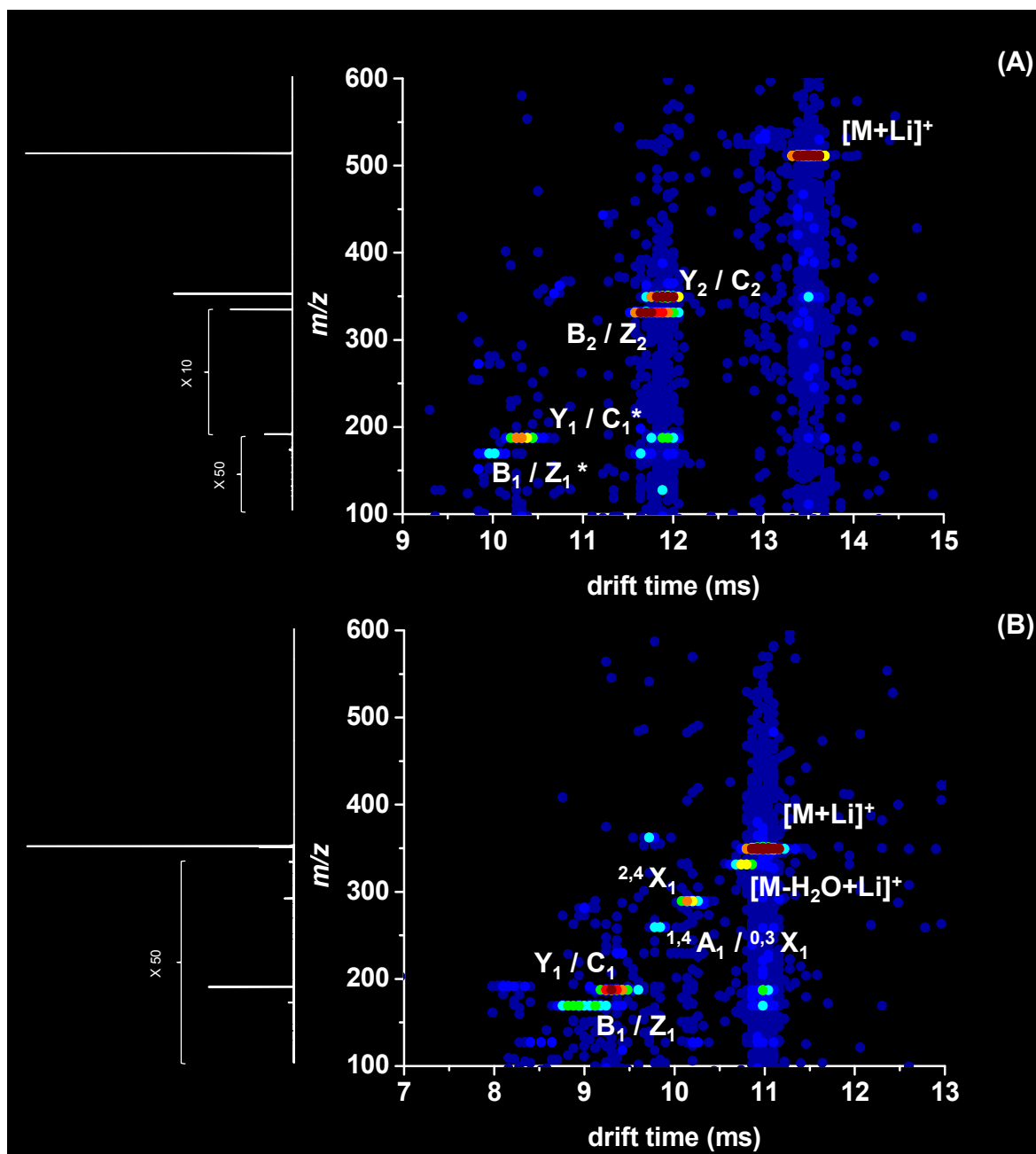
1
2
3 MS. **(b)** and **(c)** Lithiated fragment ions obtained by IMS-CID-IMS-MS (m/z 187 and m/z
4 169).
5
6
7

8
9 **Figure 5.** Mobility distributions of trisaccharides raffinose (top trace), melezitose (middle
10 trace) and maltotriose (bottom trace). **(a)** Precursor ions (m/z 511) are obtained by IMS-
11 MS. **(b)** and **(c)** Fragment ions are obtained by IMS-CID-IMS-MS (m/z 349 and m/z
12 331). All species are lithiated.
13
14
15
16
17

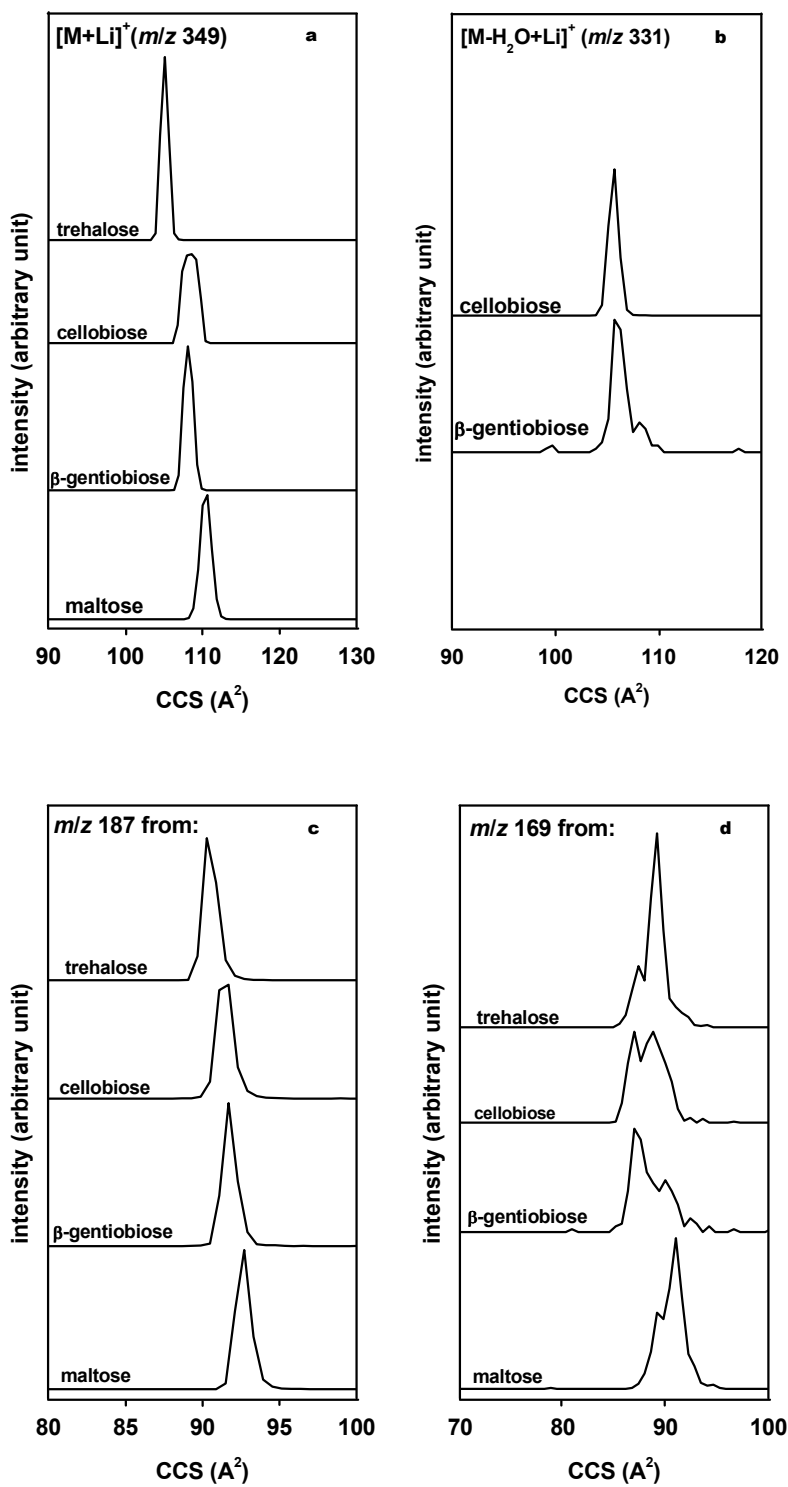
18
19 **Figure 6.** Collision cross section (ccs) of lithiated disaccharide precursor ions as a
20 function of the ccs of Y_1/C_1 (empty squares) and B_1/Z_1 (full squares) lithiated fragment
21 ions (in the case of multiple peaks, the main feature is reported). Dash lines indicate the
22 position of the precursor ion ccs in a single dimension (x-axis). The nature of the
23 monosaccharide fragment unit is represented by a color code: glucose in purple,
24 glucose or fructose in blue and glucose or galactose in green.
25
26
27
28
29
30
31
32
33
34
35
36
37
38
39
40
41
42
43
44
45
46
47
48
49
50
51
52
53
54
55
56
57
58
59
60

Gaye *et al.* Figure 1



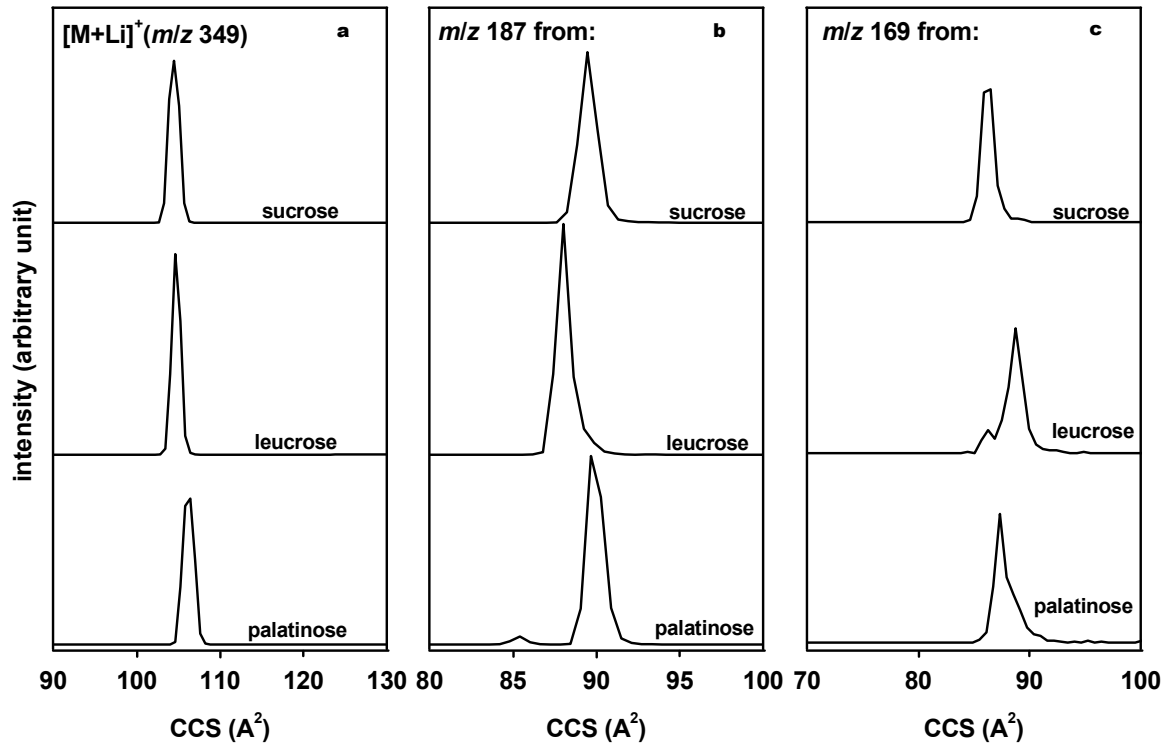
Gaye *et al.* Figure 2

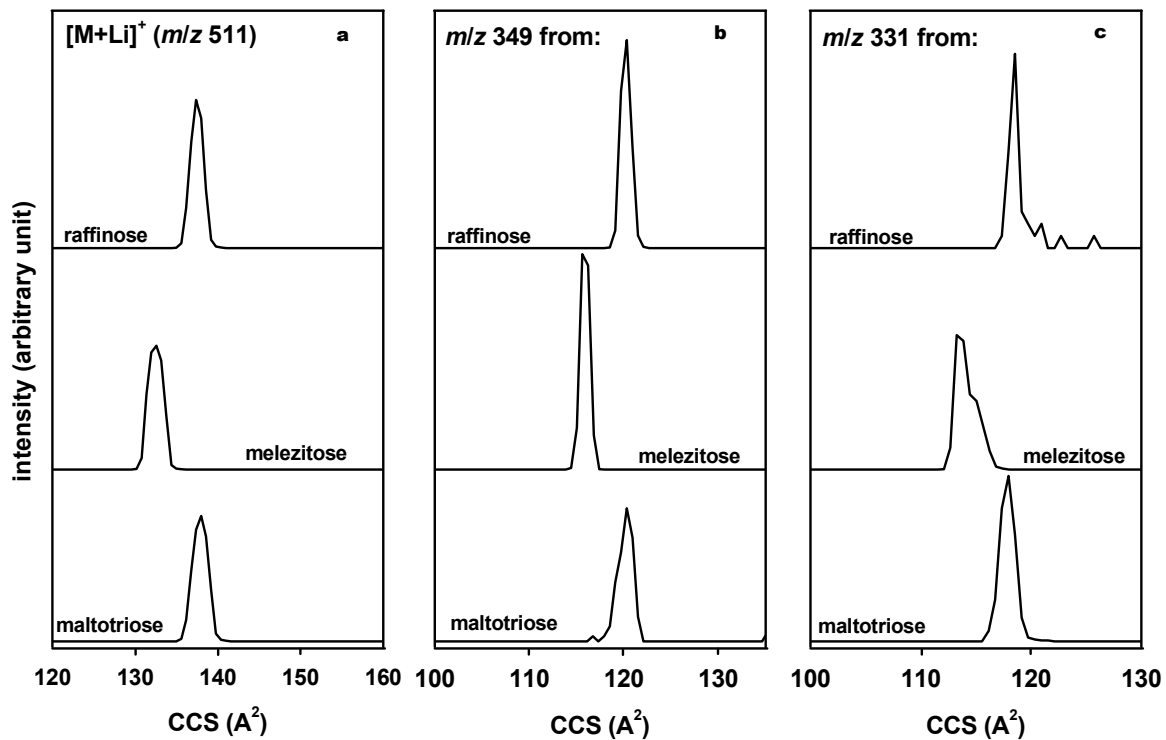
Gaye et al. Figure 3

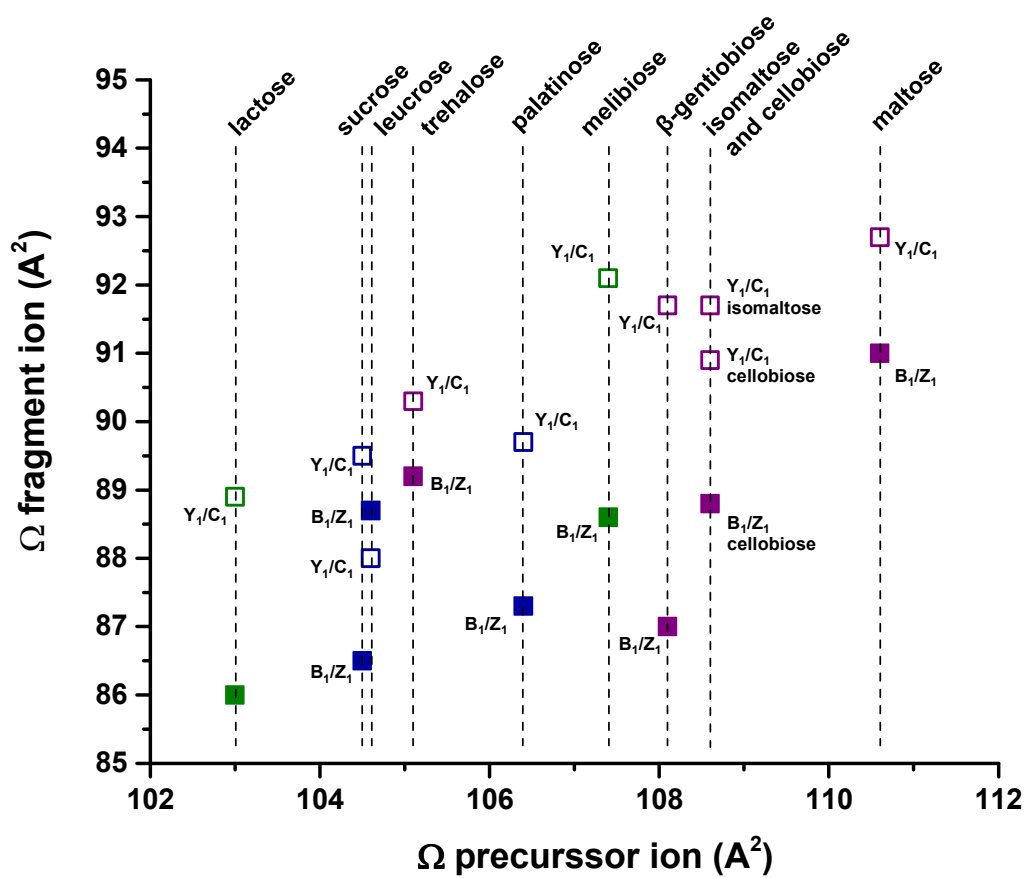


1
2
3
4
5
6
7
8
9
10
11
12
13
14
15
16
17
18
19
20
21
22
23
24
25
26
27
28
29
30
31
32
33
34
35
36
37
38
39
40
41
42
43
44
45
46
47
48
49
50
51
52
53
54
55
56
57
58
59
60

Gaye et al. Figure 4



Gaye *et al.* Figure 5

Gaye *et al.* Figure 6

References

- (1) Laine R. A. Information capacity of the carbohydrate code. *Pure & Appl. Chem.* **1997**, 69(9), 1867-1873.
- (2) Sansom, C.; Markman, O. *Glycobiology*. Scion Publishing Ltd, (2007).
- (3) Varki, A.; Cummings, R.; Esko, J.; Freeze, H.; Hart, G.; Marth, J. (editors) *Essentials of Glycobiology*. 2nd edition. CSHL Press, (2009).
- (4) Yuriev, E.; Ramsland, P. A. (editors). *Structural Glycobiology*. CRC Press, (2013).
- (5) Clemmer, D. E.; Jarrold, M. F. Ion Mobility Measurements and their Applications to Clusters and Biomolecules. *J. Mass Spectrom.* **1997**, 32, 577-592.
- (6) Hoaglund, C. S.; Valentine, S. J.; Sporleder, C. R.; Reilly, J. P.; Clemmer, D. E. Three-Dimensional Ion Mobility/TOFMS Analysis of Electrosprayed Biomolecules. *Anal. Chem.* **1998**, 70, 2236-2242.
- (7) Alley, W. R.; Novotny, M. V. Structural Glycomic Analyses at High Sensitivity: A Decade of Progress. *Annual Review of Analytical Chemistry.* **2013**, 6, 237-265.
- (8) Ruhaak, L. R.; Deelder, A.M.; Wührer, M. Oligosaccharide analysis by graphitized carbon liquid chromatography-mass spectrometry. *Analytical and Bioanalytical Chemistry.* **2009**, 394(1), 163-174.
- (9) Jiao, J.; Zhang H.; Reinhold, V. N. High performance IT-MSⁿ sequencing of glycans: Spatial resolution of ovalbumin isomers. *International Journal of Mass Spectrometry.* **2011**, 303(2-3), 109-117.

- 1
2
3
4 (10) Mittermayr, S.; Bones, J.; Guttman, A. Unraveling the Glyco-Puzzle: Glycan
5 Structure Identification by Capillary Electrophoresis. *Anal. Chem.* **2013**, 85(9), 4228-
6 4238.
7
8
9
10
11 (11) Prien, J. M.; Ashline, D. J.; Lapadula, A. J.; Zhang, H.; Reinhold, V.N. The high
12 mannose glycans from bovine ribonuclease B isomer characterization by ion trap MS,
13 *J.Am. Soc. Mass Spectrom.* **2009**, 20, 539–556.
14
15
16
17 (12) Da Costa, E. V.; Moreira, A. S. P.; Nunes, F. M.; Coimbra, M. A.; Evtuguin, D. V.;
18 Domingues, M. R. M. Differentiation of isomeric pentose disaccharides by electrospray
19 ionization tandem mass spectrometry and discriminant analysis. *Rapid Commun. Mass*
20 *Spectrom.* **2012**, 26(24), 2897-2904.
21
22
23
24 (13) Adamson, J.T.; Hakansson, K. Electron Capture Dissociation of Oligosaccharides
25 Ionized with Alkali, Alkaline Earth, and Transition Metals. *Anal. Chem.* **2007**, 79, 2901–
26 2910.
27
28
29
30 (14) Yu, X.; Huang, Y. Q.; Lin, C.; Costello, C. E. Energy-Dependent Electron Activated
31 Dissociation of Metal-Adducted Permethylated Oligosaccharides. *Anal. Chem.* **2012**,
32 84(17), 7487-7494.
33
34
35 (15) Alley, W. R. Jr.; Mechref, Y.; Novotny, M. V. Characterization of glycopeptides by
36 combining collision-induced dissociation and electron-transfer dissociation mass
37 spectrometry data. *Rapid Commun. Mass Spectrom.* **2009**, 23(1), 161-170.
38
39
40
41 (16) Han, L.; Costello, C. Electron Transfer Dissociation of Milk Oligosaccharides. *J.Am.*
42 *Soc. Mass Spectrom.* **2011**, 22(6), 997-1013.
43
44
45
46
47
48
49
50
51
52
53
54
55
56
57
58
59
60

- 1
2
3
4 (17) Devakumar, A.; Thompson, M.S.; Reilly, J.P. Fragmentation of oligosaccharide
5 ions with 157 nm vacuum ultraviolet light, *Rapid Commun. Mass Spectrom.* **2005**, 19,
6 2313–2320.
7
8
9
10
11 (18) Wilson, J.J.; . Brodbelt, J.S. Ultraviolet photodissociation at 355 nm of
12 fluorescently labeled oligosaccharides. *Anal. Chem.* **2008**, 80, 5186–5196.
13
14
15 (19) Lee, S.; Valentine, S. J.; Reilly, J. P.; Clemmer, D. E. Analyzing a Mixture of
16 Disaccharides by IMS–VUVPD–MS. *Int. J. Mass Spectrom.*, **2012**, 309, 161–167.
17
18
19 (20) Zhu, M.; Bendiak, B.; Clowers, B.; Hill, H. H. Jr. Ion mobility-mass spectrometry
20 analysis of isomeric carbohydrate precursor ions. *Analytical and Bioanalytical*
21 *Chemistry.* **2009**, 394(7), 1853-67.
22
23
24
25
26 (21) Aoki-Kinoshita, K. F. Glycome Informatics. CRC Press, Taylor & Francis Group
27
28
29
30
31
32
33 (22) Liu, Y.; Clemmer, D. E. Characterizing Oligosaccharides Using Injected–Ion
34 Mobility/Mass Spectrometry, *Anal. Chem.* **1997**, 69, 2504–2509.
35
36
37 (23) Isailovic, D. ; Kurulugama, R. T.; Plasencia, M. D.; Stokes, S. T.; Kyselova, Z.;
38 Goldman, R.; Mechref, Y.; Novotny, M. V.; Clemmer, D. E. Profiling of human serum
39 glykans associated with liver cancer and cirrhosis by IMS-MS. *J. Proteome Res.* **2008**,
40 7, 1109-1117.
41
42
43
44
45 (24) Plasencia, M. D. ; Isailovic, D. ; Merenbloom, S. I. ; Mechref, Y. ; Clemmer, D. E.
46 Resolving and Assigning N-linked Glycan Structural Isomers from Ovalbumin by IMS-
47 MS. *J. Am. Soc. Mass Spectrom.* **2008**, 19(11), 1706-1715.
48
49
50
51
52
53
54
55
56
57
58
59
60

- 1
2
3
4 (25) Zucker, S. M.; Lee, S.; Webber, N.; Valentine, S. J.; Reilly, J. P. and Clemmer, D.
5
6 E. An Ion Mobility/Ion Trap/Photodissociation Instrument for Characterization of Ion
7
8 Structure. *J. Am. Soc. Mass Spectrom.*, **2011**, 22, 1477–1485.
9
10
11 (26) Zhu, F.; Lee, S.; Valentine, S. J.; Reilly, J. P.; Clemmer, D. E. Mannose7 Glycan
12
13 Isomer Characterization by IMS-MS/MS Analysis. *J. Am. Soc. Mass*
14
15 *Spectrom.*, **2012**, 23, 2158–2166.
16
17
18 (27) Lee, S.; Wyttenbach, T.; Bowers, M. T.; Gas phase structures of
19
20 sodiated oligosaccharides by ion mobility ion chromatography methods. *International*
21
22 *Journal of Mass Spectrometry*. **1997**, 167, 605-614.
23
24
25 (28) Clowers, B. H.; Dwivedi, P.; Steiner, W. E.; Hill, H. H. Jr.; Bendiak, B. Separation of
26
27 sodiated isobaric disaccharides and trisaccharides using electrospray ionization-
28
29 atmospheric pressure ion mobility-time of flight mass spectrometry. *J. Am. Soc. Mass*
30
31 *Spectrom.* **2005**, 16(5), 660-669.
32
33
34 (29) Dwivedi, P.; Bendiak, B.; Clowers, B. H.; Hill, H. H. Jr. Rapid resolution of
35
36 carbohydrate isomers by electrospray ionization ambient pressure ion mobility
37
38 spectrometry-time-of-flight mass spectrometry (ESI-APIMS-TOFMS). *J. Am. Soc. Mass*
39
40 *Spectrom.* **2007**, 18(7), 1163-1175.
41
42
43 (30) Zhu, M.; Bendiak, B.; Clowers, B.; Hill, H. H. Jr. Ion mobility-mass spectrometry
44
45 analysis of isomeric carbohydrate precursor ions. *Analytical and Bioanalytical*
46
47 *Chemistry*. **2009**, 394(7), 1853-67.
48
49
50 (31) Williams, J. P.; Grabenauer, M.; Holland, R. J.; Carpenter, C. J.; Wormald, M. R.;
51
52 Giles, K.; Harvey, D. J.; Bateman, R. H.; Scrivens, J. H.; Bowers, M. T.;
53
54
55
56
57
58
59
60

1
2
3
4
5 mixtures by ion mobility mass spectrometry. *Int. J. Mass Spectrom.* **2010**, 298(1-3),
6
7 119-127.

8
9 (32) Fenn, L. S.; McLean, J. A.. Structural resolution of carbohydrate positional and
10
11 structural isomers based on gas-phase ion mobility-mass spectrometry. *Phys. Chem.*
12
13 *Chem. Phys.* **2011**, 13(6), 2196-2205.

14
15 (33) Harvey, D. J.; Scarff, C. A.; Edgeworth, M.; Crispin, M.; Scanlan, C. N.; Sobott, F.;
16
17 Allman, S.; Baruah, K.; Pritchard, L.; Scrivens, J. H. Travelling wave ion mobility and
18
19 negative ion fragmentation for the structural determination of N-linked glycans.
20
21 *Electrophoresis.* **2013**, 34(16), 2368-2378.

22
23 (34) Li, H. L.; Bendiak, B.; Siems, W. F.; Gang, D. R.; Hill, H. H. Jr. Carbohydrate
24
25 Structure Characterization by Tandem Ion Mobility Mass Spectrometry (IMMS)². *Anal.*
26
27 *Chem.* **2013**, 85(5), 2760-2769.

28
29 (35) Huang, Y. T.; Dodds, E. D. Ion Mobility Studies of Carbohydrates as Group I
30
31 Adducts: Isomer Specific Collisional Cross Section Dependence on Metal Ion Radius.
32
33 *Anal. Chem.* **2013**. 85(20), 9728-9635.

34
35 (36) Both, P.; Green, A. P.; Gray, C. J.; Šardžík, R.; Voglmeir, J.; Fontana, C.;
36
37 Austeri, M.; Rejzek, M.; Richardson, D.; Field, R. A.; Widmalm, G.; Flitsch, S. L.; Evers,
38
39 C. E. Discrimination of epimeric glycans and glycopeptides using IM-MS and its
40
41 potential for carbohydrate sequencing. *Nature Chemistry.* **2014**, 6, 65–74.

42
43 (37) Collins, D. C; Lee, M. L. Developments in ion mobility spectrometry-mass
44
45 spectrometry. *Analytical and Bioanalytical Chemistry.* **2002**, 372(1), 66-73.

46
47 (38) valentine, S. J. Developing liquid chromatography ion mobility mass spectrometry
48
49 techniques. *Expert Rev. Proteomics.* **2005**, 553-565.

1
2
3
4 (39) Koeniger, S. L.; Merenbloom, S. I.; Valentine, S. J.; Jarrold, M. F.; Udseth, H.;
5
6 Smith, R.; Clemmer, D. E. An IMS-IMS Analogue of MS-MS. *Anal. Chem.* **2006**, 78,
7
8 4161-4174.
9

10
11 (40) Merenbloom, S. I. ; Koeniger, S. L. ; Bohrer, B. C. ; Valentine, S. J. ; Clemmer, D.
12
13 E. Improving the Efficiency of IMS-IMS by a Combing Technique. *Anal. Chem.* **2008**,
14
15 80(6), 1918-1927.
16

17
18 (41) Merenbloom, S. I.; Koeniger, S. L.; Valentine, S. J.; Plasencia, M. D.; Clemmer, D.
19
20 E. IMS–IMS and IMS–IMS–IMS/MS for Separating Peptide and Protein Fragment
21
22 Ions, *Anal. Chem.* **2006**, 78, 2802–2809.
23

24
25 (42) DOMON, B.; COSTELLO, C. E. A systematic nomenclature for carbohydrate
26
27 fragmentations in FAB-MS MS spectra of glycoconjugates. *Glycoconjugate journal.*
28
29 **1988**, 5(4), 397-409.
30

31
32 (43) Mason, E. A., McDaniel, E. W.; *Transport Properties of Ions in Gases*; Wiley: New
33
34 York, 1988.
35

36
37 (44) Revercomb, H. E.; Mason, E. A. Theory of plasma chromatography/gaseous
38
39 electrophoresis. Review. *Anal. Chem.* **1975**. 47(7), 970-983.
40
41
42
43
44
45
46
47
48
49
50
51
52
53
54
55
56
57
58
59
60